Energy, exergy, thermoeconomic and sustainability assessment of tire pyrolysis oil in common rail direct injection diesel engine

Haseeb Yaqoob[a,b], Yew Heng Teoh[a], Muhammad Ahmad Jamil[c], Farooq Sher[d,*]

[a] *School of Mechanical Engineering, Universiti Sains Malaysia, Engineering Campus, 14300 Nibong Tebal, Penang, Malaysia*

[b] *Department of Mechanical Engineering, Khwaja Fareed University of Engineering and Information Technology, Rahim Yar Khan 64200, Pakistan*

[c] *Department of Mechanical and Construction Engineering, Northumbria University, Newcastle Upon Tyne, NE1 8ST, UK*

[d] *Department of Engineering, School of Science and Technology, Nottingham Trent University, Nottingham NG11 8NS, UK*

*Corresponding author:
Dr. F. Sher
Assistant Professor
Department of Engineering, School of Science and Technology
Nottingham Trent University
Nottingham
NG11 8NS
UK
E-mail address: Farooq.Sher@ntu.ac.uk (F.Sher)
Tel.: +44 (0) 115 84 86679

Abstract

Waste to fuel conversion has attracted prominence due to higher fuel demand, waste disposal issues, and environmental and economic impact. Therefore, an alternative approach for addressing the issue of waste tire disposal can be provided by using tire pyrolysis oil (TPO). The energy, exergy, thermoeconomic and sustainability studies of TPO-diesel blends were carried out in this study. The analysis was compared with biodiesel-diesel blended fuel and pure diesel. DP10 (Diesel 90%-TPO 10%), DB10 (Diesel 90%-Biodiesel 10%), and neat diesel are used in the experimental study. The four-cylinder diesel engine was used to perform the experiments at different crankshaft speeds ranges 1000-3500 rpm with the increment of 500 rpm. The results reveal that at 3000 rpm, DP10 shows the highest energy and exergy efficiency, 37.12% and 39.60%, respectively, compared to DB10 and D100. The thermoeconomic study indicates that DP10 produced the lowest energy and exergy losses compared to DB10 and D100. The DP10 provides the highest sustainability index, demonstrating that the DP10 is the most sustainable fuel compared to D100 and DB10. It is concluded that the DP10 shows the best results, and it is appropriate to use in the turbocharged common-rail direct injection diesel engine.

Keywords: Renewable energy; Alternative fuels; Tire pyrolysis oil; Biodiesel; Thermoeconomic; CO_2 reduction and Combustion.

44 Nomenclature

C_p	specific heat capacity (kJ/kg. K)
DN	depletion Number
$E\dot{n}$	energy rate (kW)
ex	specific exergy rate (kJ/kg)
h	specific enthalpy (kJ/kg)
H_u	lower heating value (kJ/kg)
IP	improvement potential (kW)
K	cost ($)
$\dot{m}$	mass flow rate (kg/s)
n	engine speed (rpm)
P	pressure (kPa)
R	thermoeconomic parameter (kW/$)
$\bar{R}$	universal gas constant (kJ/kmol.°°K)
SI	sustainability index
T	torque (Nm) and temperature (K)
$\dot{V}$	volumetric flow rate (m^3/s)
y	molar fraction (%)

Greek Symbol

ε	chemical exergy factor
ρ	density (kg/m^3)
η	energetic efficiency (%)
ψ	exergetic efficiency (%)
ω	angular velocity (rad/s)

Abbreviations

ASTM	American society for testing materials
B100	clean palm biodiesel
BSFC	brake specific fuel consumption
BTDC	bottom dead center
BTE	brake thermal efficiency
CO	Carbon monoxide
CO_2	Carbon dioxide

CI	compression ignition
CO_2	carbon dioxide
D100	neat diesel (100% diesel)
DB10	diesel 90%-biodiesel 10%
DP10	diesel 90%-Tire pyrolysis oil 10%
EXCEM	exergy cost energy mass method
HC	hydrocarbons
HRR	heat release rate
ICEs	internal combustion engines
N	nitrogen
NO_x	oxides of nitrogen
nPAH	nitric polycyclic aromatic hydrocarbons
PAH	polycyclic aromatic hydrocarbons
PM	particulate matter
PN	particular number
O	Oxygen
SDGs	global sustainable development goals
SO_2	sulfur dioxide
TPO	tire pyrolysis oil
UHC	unburned hydrocarbon

Subscripts

air	air
cap	capital
dest	destruction
en	energy
ex	exergy
exh	exhaust
fuel	fuel
gen	generation
in	inlet
loss	loss
out	outlet
OCC	other

O-M	operation and maintenance
w	work
o	environmental state

1. Introduction

Fuel demand continues to rise because of the exponential growth of automotive vehicles in the transport sector [1]. In the meantime, global petroleum supplies are increasingly depleting, and public concern about global climate change has consequently been raised, urging several kinds of research on alternative energy resources. Compared to conventional petroleum-based gasoline, biofuels have a substantial advantage in environmental sustainability and renewability [2]. It is because, during the combustion process, biofuels reduce emissions [3] that are harmful like carbon dioxide (CO_2), carbon monoxide (CO), soot emissions, and unburned hydrocarbon (UHC) [4]. Therefore, it is not surprising that the two forms of alternative economic biofuels, biodiesel and tire pyrolysis oil (TPO), have already gotten significant attention from researchers.

Due to its significant benefits and advantages, biodiesel as an alternative fuel has gained broad acceptance as a substitute for petroleum-based fuels used in diesel engines. Its essential properties are comparable or better than diesel fuel, such as its biodegradable, non-toxic, flash point, and cetane number. Besides, it is an impressive replacement fuel that presents the least challenge in securing health impact control requirements [5]. Biodiesel is diesel-compatible and can be combined with diesel fuel in varying quantities to produce a robust biodiesel blend or can be used directly in existing diesel engines without the need for a comprehensive engine modification. Biofuels may be made from a variety of different sources. Biodiesel is an alternative fuel that may be made from plant oils, vegetable oils, and animal fats (both edible and non-edible) [6], etc., through transesterification, one of the most efficient and appropriate methods [7,8].

As an alternative to conventional diesel fuel, tire pyrolysis oil (TPO) extracted from scrap tires offers various capabilities [9,10]. Pyrolysis involves a method of oxygen-free thermal decomposition with the additional benefit of reprocessing waste rubber and reducing reliance on natural resources [11,12], where the organic component (rubber) decomposes at a temperature of 500 °C to produce oil, coal, and char content in addition to the recovery of steel. The oil produced can be directly used as fuel, upgraded using catalysts to a premium grade fuel, applied to petroleum refinery stocks, or used to generate hydrogen [13]. TPO provides the necessary sustainable solution to the ever-growing quantity of waste rubber and tires created by the processing and automotive industries without raising the earth's waste burden [14,15]. It is estimated that ~1.5 billion waste tires are generated worldwide annually [16]. It is not easy to dispose of them since they are non-biodegradable and ultimately help as collateral pollutants [17,18].

Tires are 21.5-35 wt.% made of carbon and 45-65 wt.% of black rubber, and 16.5-25 wt.% of steel. Zinc, sulfur, and additives are also included [19]. The 35-40 MJ/kg higher calorific value [20] and a significant quantity of carbon black in the rubber for the vehicle tire show a suitable fuel production feedstock. Some experimental investigations are mentioned to use waste TPO (as an alternative fuel) to diesel [11,13]. Exergy is an energy quality indicator that addresses the maximum amount of work generated by a system exposed to the environment or works with the minimum amount needed to reach the given state based on environmental conditions. The system's irreversibilities are included in exergy analysis; thus, it offers more detailed thermal systems results than an energy assessment [21]. In this context, several studies have been conducted in the literature on the exergy study of internal combustion engines (ICEs). Karagoz et al. [22] performed the energy, exergy, sustainability, and economic assessment for diesel and blends of tire pyrolysis oil with diesel fuel on a compression ignition engine, four strokes having single-cylinder and at different engine torques. It is studied that the highest efficiency values of energy and exergy are found for TPO10D90 28.15% and 26.36% as compared to clean diesel 26.89% and 25.19%, respectively.

The highest value of sustainability index for TPO10D90 at 12 Nm torque is found 1.35 while the lowest value of sustainability index for clean diesel is noticed at 1.33. At fixed speeds (1800 rpm) and various loads, Mori and Caliskan [23] studied the energy, exergy, thermoeconomic, and sustainability analysis for the diesel engine when fueled with biodiesel-diesel blends and diesel. The efficiency of energy and exergy for blended fuel of diesel-biodiesel is greater than diesel fuel, however, these parameters are improved as the biodiesel content increases. Ozdalyan et al. [24] conducted an exergy study on four cylinders, spark-ignition engines at various speeds. The highest energy and exergy efficiencies at 2500 rpm were 29.78% and 27.77%, respectively. Karthickeyan et al. [25] conducted energy and exergy studies of the pomegranate seed oil methyl ester as a fuel in ceramic coated diesel engines at optimal operating parameters. The exergy destruction value is 46.07% for the thermal barrier coated engine having a compression ratio of 19.5:1, 45.95% for the injection pressure at 240 bar, and 46.19% for the injection timing of 25° BTDC.

Paul et al. [26] recorded that a compression ignition (CI) engine can obtain a 25.64% rise in exergy performance, a 22.02% reduction in exergy destruction, and a 21.06% of decline in generation of entropy as compared to diesel fuel when the engine is fueled by diesel-ethanol-pongamia pinata methyl ester blended fuel with the 35, 15, and 50% respectively. The study of sustainability measures the capacity to maintain a system. Sustainability aims to include the specifications of the existing concerning the benefits of the future. In the literature, there are numerous studies combining sustainability research with exergy analysis for several fields and processes [27,28]. Aghbashlo et al. [29] examined the efficiency of energy and sustainability of a diesel engine fueled with waste oil biodiesel and extracted from blends of whitening earth-diesel having expanded polystyrene. The test engine was run with a biodiesel-diesel blend consisting of expanded polystyrene of 50 g, the calculated sustainability index 1.67, and the test engine's efficiency of 40.21%. Furthermore, Sharma et al. [30] stated that the diesel engine's optimum input data-fueled with jojoba biodiesel-diesel blends were estimated to be 21.52 MPa injection pressure, injection timing 25° BTDC, jojoba biodiesel fuel share 24%, and engine load of 80% as sustainability.

The focus of present study is on the use of TPO as a fossil fuel alternative in turbocharged common-rail direct injection (CRDI) diesel engine. The lower-level blending of up to 10% with fossil diesel fuel is included in this study. A lower-level blend in diesel engines can be operated, which effectively needs little to no change, whereas biodiesel/TPO has identical properties to diesel fuels. Further explanation for it is the TPO's potential to be a sustainable alternative for producing non-food transportation fuels versus problems with fuel or the use of valuable agricultural land. Consequently, fellow investigators are allowed to participate with acceptable alternative fuels based on non-edible feedstock. The continuous use of edible fuel sources will negatively influence the food industry and cause environmental problems. Besides, the object of the comparative assessment of the energy, exergy, thermoeconomic, and sustainability parameters of the TPO-diesel and biodiesel-diesel blends in turbocharged direct-injection common-rail engines will be to distinguish between better alternative fuels.

2. Experimental

2.1. Test fuels

Steel wires are removed from waste tires, and only a shredded tire is used in the pyrolysis process. These small tire parts are reacted in a thermal chamber during the pyrolysis process. In fluid tire pyrolysis oil formation, the pyrolysis chamber's reaction temperature increases from 400 °C to 600 °C. The tire pyrolysis oil, palm biodiesel (B100), and diesel fuel are procured from Malaysia's local company. The physicochemical properties of the TPO have been determined based on the ASTM standards. Subsequently, a magnetic stirrer is used to prepare the DP10 (90% diesel, 10% TPO) and B10 (10% biodiesel, 90% diesel) fuel blends. **Table 1** displays the significant physical properties of DP10, B10, neat TPO (P100), diesel, and neat biodiesel (B100). Interestingly, it is found that a TPO has a higher calorific value than biodiesel, however with a marginally lower calorific value than diesel fuel, which means that TPO is providing an acceptable diesel fuel replacement for diesel engines, and it can be an alternative fuel like biodiesel.

2.2. Test engine operating conditions

A diesel engine with a four-cylinder with a direct-injection turbocharger operating by injection system named common-rail used for test engine is shown in **Fig. 1.** The equipment used for this research was arranged and set up. **Table 2** shows the engine testbed specifications. The engine has a maximum power of 45 kW and a maximum torque of 160 Nm, while the common-rail injection system requires a maximum injection pressure of 140 MPa to operate. The full-load curve was used to assess the engine's performance parameters in this investigation. The engine is run at full load to offer a clear study of the influence of various fuel blends on engine operating characteristics. It is because engines require maximum fuel rates at full load (maximum power). In addition, the engine speed is adjusted in 500-rpm increments from 1000 to 3500 rpm. These six engine speeds were chosen to indicate a wide range of engine operating ranges under full load circumstances. At full load, the engine's torque and braking power were measured using an eddy current dynamometer. Meanwhile, a gas analyzer (AVL DiGas 4000 for gaseous emission measurement) analyzed exhaust gas emissions exposed to gas analyzers directed from the engine.

2.3. Uncertainty analysis

The uncertainty analysis is performed by **Eq. (1)**, which gives the total value of this system's uncertainty [31].

$$W_R = [(\frac{\partial R}{\partial x_1} w_1)^2 + (\frac{\partial R}{\partial x_2} w_2)^2 + ...(\frac{\partial R}{\partial x_n} w_n)^2]^{\frac{1}{2}} \qquad (1)$$

where, w shows the dimension of shape factor W_R (%) represents system uncertainty, R represents total function uncertainty, while n shows the total number of independent variables involved in the experiment. The detailed list of measurement type, range, accuracy, technique, and percentage uncertainty is given in **Table 3.** This study's total uncertainty is calculated to be 1.77%, and that value is within the acceptable limit.

3. Theoretical methods

The experimental data collected from the engine testbed is given in **Table S1**. While performing all the studies mentioned above following assumptions were considered. (1) The engine is operating in a steady state, having a steady flow. (2) The exhaust gases exposed to the environment and supplied air to the engine are ideal. (3) The kinetic and potential energy and kinetic and potential exergy of the system are changed negligibly. (4) The dead state pressure (P_0) and temperature (T_0) are assumed to be 101 kPa and 288.15 K, respectively.

3.1. Energy analysis

Fig. 2 depicts the thermodynamic energy balance for control volume with all parameters in the diesel engine taken into account [25]. The law of conservation of energy does the energy balance and when the system is in steady-state and is stated in **Eq. (2)**.

$$\sum E\dot{n}_{in} = \sum E\dot{n}_{out} \tag{2}$$

Using Eq. (2), the energy balance for this study is written using **Eq. (3).**

$$E\dot{n}_{air} + E\dot{n}_{fuel} = E\dot{n}_{w} + E\dot{n}_{exh} + E\dot{n}_{loss} \tag{3}$$

Here $E\dot{n}_{air}$ is the air supplied energy rate of the test engine, $E\dot{n}_{fuel}$ shows the fuel provided energy rate for the test engine, $E\dot{n}_{w}$ represents the work's energy rate generated by the test engine, $E\dot{n}_{exh}$ shows the gases energy rate exhausted by the engine testbed and directed to the environment and $E\dot{n}_{loss}$ represents the energy loss rate due to the engine's heat transfer and directed to the environment. This 1st term air energy rate could be calculated as shown in **Eq. (4).**

$$E\dot{n}_{air} = \dot{m}_{air} h_{air} = \rho_{air} \dot{V}_{air} h_{air} \tag{4}$$

where h, ρ, $\dot{m}$ and $\dot{V}$ are representing the specific enthalpy, density, mass flow rate, and volume flow rate of air, respectively. The supplied fuel energy rate for the test engine could be calculated using **Eq. (5).**

$$E\dot{n}_{fuel} = \dot{m}_{fuel} H_u \tag{5}$$

Here, H_u represents the fuel's lower heating values. The following **Eq. (6)** can calculate the work-energy rate produced by the test engine.

$$E\dot{n}_w = \omega T \tag{6}$$

where T, ω is the torque and angular velocity of a test engine, respectively, and angular velocity of test engine is found using **Eq. (7).**

$$\omega = \frac{2\pi n}{60} \tag{7}$$

where n shows the angular speed of the crankshaft, the following **Eq. (8)** can find the rate of energy of gases exhausted from the test engine to the surroundings [22].

$$E\dot{n}_{exh} = \sum_{i=1}^{n} \dot{m}_i h_i = \dot{m}_{CO} h_{CO} + \dot{m}_{NO_x} h_{NO_x} + \dot{m}_{CO_2} h_{CO_2} + ... \tag{8}$$

where h_i, $\dot{m}_i$ are the specific enthalpy and mass flow rate of exhaust gases, respectively. Once all the terms involved in **Eq. (3)** are calculated, then the $E\dot{n}_{loss}$ is calculated by this energy balance **Eq. (3)**. Energy efficiency is calculated using **Eq. (9).**

$$\eta_{en} = \frac{E\dot{n}_w}{E\dot{n}_{air} + E\dot{n}_{fuel}} \tag{9}$$

3.2. Exergy analysis

The total energy utilization cannot be accomplished by only considering the energy analysis [32]. It does not give information about the quality and the usefulness of all streams of energy that are exiting in the form of product and waste and crossing the system's boundary [33]. Exergy analysis is important for evaluating a significant change in the working environment [34]. Exergy, unlike energy, is a non-conserved and destroyable resource. Therefore, a new term, exergy destruction, will be introduced in the steady-state exergy balance system. Exergy balance for the systems of steady-state is stated using **Eq. (10).**

$$\sum E\dot{x}_{in} = \sum E\dot{x}_{out} + \sum E\dot{x}_{dest} \tag{10}$$

Eq. (11) of exergy balance could be expressed Eq. (11).

$$E\dot{x}_{air} + E\dot{x}_{fuel} = E\dot{x}_{w} + E\dot{x}_{exh} + E\dot{x}_{loss} + E\dot{x}_{dest} \tag{11}$$

Where $E\dot{x}_{air}$, $E\dot{x}_{fuel}$, $E\dot{x}_{exh}$, $E\dot{x}_{w}$, $E\dot{x}_{dest}$ and $E\dot{x}_{loss}$ are the exergy rates of air supplied, fuel supplied, gases from the exhaust system are discharged into the air, work generated by the test engine, exergy destruction rate, and exergy loss rate, respectively. Supplied air exergy rate for the test engine is measured by using the specified **Eq. (12)**.

$$E\dot{x}_{air} = \dot{m}_{air} c_{p,air} [(T_{air} - T_0) - T_0 \ln(\frac{T_{air}}{T_0})] \tag{12}$$

where T, c_p signifies the temperature and specific heat, respectively. Fuel supplied exergy rate for the test engine is measured by using the given **Eq. (13).**

$$E\dot{x}_{fuel} = \dot{m}_{fuel} H_u \varepsilon_{fuel} \tag{13}$$

where ε_{fuel} is the chemical exergy factor and is calculated using **Eq. (14)** [35].

$$\varepsilon_{fuel} = 1.0401 + 0.1728\frac{H}{C} + 0.0432\frac{O}{C} + 0.2169\frac{\alpha}{C}[1 - 2.0628\frac{H}{C}] \tag{14}$$

where α , C, H, and O represent the sulfur content, mass ratios of carbon, hydrogen, and oxygen, respectively in the different fuels. These elements' (C, α , O, and H) mass fractions are listed in **Table 4** and determined through ultimate analysis. The energy rate and exergy rate of work are equal. Therefore, the exergy rate generated by work for the test engine could be calculated using **Eq. (15).**

$$E\dot{x}_w = E\dot{n}_w = \omega T \tag{15}$$

Furthermore, exhaust gases exergy rate is calculated by using the given **Eq. (16)**.

$$E\dot{x}_{exh} = \sum_{i=1}^{n} \dot{m}_i (ex_{tm,i} + ex_{ch,i}) \tag{16}$$

where $ex_{tm,i}$ is the specific physical and $ex_{ch,i}$ is the specific chemical exergy rates for the exhaust gases. For i_{th} compound, the $ex_{ch,i}$ and $ex_{tm,i}$ of exhaust gases is calculated by using **Eq. (17)** and **Eq. (18)** respectively:

$$ex_{tm,i} = C_{p,i}[(T_{exh} - T_0) - T_0 \ln(\frac{T_{exh}}{T_0})] \tag{17}$$

$$ex_{ch,i} = \bar{R} T_0 \ln(\frac{y_i}{y_{env,i}}) \tag{18}$$

where T_{exh} $\bar{R}$, T_0, y_i, $y_{env,i}$ and $ex_{ch,i}$ represents the exhaust gases temperature, Universal gas constant, i_{th} compound molar fraction for exhaust gases, the i_{th} compound molar fraction of environment, respectively. **Table 5** represents the values of $y_{env,i}$ [36]. For the test engine, the exergy rate of loss energy rate is calculated by using the given **Eq. (19)**.

$$E\dot{x}_{loss} = E\dot{n}_{loss}(1 - \frac{T_o}{T_{engine}}) \tag{19}$$

where T_{engine} represents the test engine block temperature. The exergy destruction rate is calculated after determining all the terms involved in **Eq. (11).** For the test engine bed, the value of exergy efficiency is calculated using the given **Eq. (20)** [22].

$$\psi = \frac{E\dot{x}_w}{E\dot{x}_{air} + E\dot{x}_{fuel}} \tag{20}$$

3.3. Thermoeconomic analysis

Thermoeconomic deals with the combination of economics and thermodynamics. The Exergy Cost Energy Mass Method (EXCEM) provides thermoeconomic analysis reported in the literature that was first provided by Rosen and Dincer in 2003 [37]. According to the EXCEM method, the **Eq. (21)** of cost balance for this analysis is stated as [22].

$$K_{in} = K_{gen} - K_{out} = \Delta K \tag{21}$$

Here, K_{gen} represents the cost of generation, and this term involves the expenditures and capital costs like a cost on maintenance and operation. The **Eq. (22)** is used to find out cost generation [22].

$$K_{gen} = K_{cap} - K_{O-M} - K_{OCC} \tag{22}$$

where K_{O-M}, K_{cap}, and K_{OCC} represent the operational and maintenance cost, capital cost, and other costs, respectively. The thermoeconomic analysis aims to give information on the relation between capital cost and energy loss. This relation is written as **Eq. (23)** [38].

$$R_{en,loss} = \frac{E\dot{n}_{loss}}{K_{cap}} \tag{23}$$

where $R_{en,loss}$ represents the thermoeconomic parameter which gives the value of total energy loss over capital investment value. Furthermore, the relation of exergy loss and exergy destruction with capital investment value is found by **Eq. (24)** and **Eq. (25)** respectively [33].

$$R_{ex,loss} = \frac{E\dot{x}_{loss}}{K_{cap}} \tag{24}$$

$$R_{ex,dest} = \frac{E\dot{x}_{dest}}{K_{cap}} \tag{25}$$

where $R_{ex,loss}$ and $R_{ex,dest}$ are the important values that give the value of exergy loss per capital investment cost and the exergy destruction per capital investment cost respectively.

3.4. Sustainability analysis

Sustainability targets to satisfy existing needs without reducing the potential of future ages to fulfil their demands. Sustainability is dependent on the conservation of the environment, social extension as well as economic buildout. With the effective use of energy assets, sustainability development can be accomplished. Because of the achievement of sustainable development, energetic and exergy efficiencies of systems are significant factors. In this report, some of the parameters have been implemented to assess the process's sustainability. Furthermore, the improvement potential (IP) will also have been included in this method. If the process irreversibility is diminished and it may be measured very well, then the exergy IP of any process can represent the IP. It may be determined by the following **Eq. (26)** [39].

$$I\dot{P} = (1-\psi)(E\dot{x}_{in} - E\dot{x}_{out}) \tag{26}$$

The depletion number is other parameter of sustainability. The depletion number (DN) **Eq. (27)** plays a significant role to calculate the fossil fuels consumption efficiency [40], which has been written below.

$$DN = \frac{E\dot{x}_{dest}}{Ex_{in}} = (1-\psi) \tag{27}$$

Another significant parameter is the sustainability index (SI), which is determined by taking depletion number inverse [38], which is written as **Eq. (28).**

$$SI = \frac{1}{DN} \tag{28}$$

4. Results and discussion

4.1. Energy analysis

The obtained results from energy analysis of blend fuels and diesel fuel are shown in **Table S2**. It was observed that an increase in rpm of the test engine increases the fuel energy rate delivered to the test engine. The energy rate of D100 fuel is always higher than the DP10 and DB10 for each test engine speed. For instance, at 2000 rpm, the fuel energy rates of D100, DB10, and DP10 were 76.81, 76.40, and 74.81 kW, respectively. Similarly, the rate of energy loss for each fuel increases with increasing rpm. At 2000 rpm, energy loss rates for D100, DB10, and DP10 were determined to be 54.50, 54.25, and 51.95 kW, respectively. The variations of energy efficiency to the engine speed of the test engine for D100, DB10, and DP10 are shown in **Fig. 3.** These investigations show as the number of test engine speed increases, each fuel energy efficiency also increases. For any test engine speed, the lowest energy efficiency among this fuel was obtained for D100, whereas it was highest for DP10. At 2000 rpm, the energy efficiency for D100, DB10, and DP10 was determined to be 33.10, 33.18, and 34.59%, respectively. The D100 has a higher energy loss to exhaust gases. The addition of hydrogen significantly increases the availability of exhaust gases [41]. Pote et al. [42] revealed the TPO-diesel blend has higher brake power (BP) and brake thermal efficiency (BTE) than diesel fuel because TPO has a higher density than diesel fuel. Due to this, DP10 shows the best performance in terms of energy efficiency.

4.2. Exergy analysis

Exergy is the highest available energy and is based on the second law of thermodynamics [21]. In this study, the test engine's exergy analysis for different fuels is shown in **Table S3**. The exergy rate value increases as the rpm of the test engine increase. The exergy rate of D100 was 37.85 kW at 1000 rpm, and 113.7 kW at 3500 rpm. The maximum fuel exergy values were noticed for D100. The exergy loss rate value for all these fuels increases with the test engine's rpm increases. Exergy loss rate at 1500 rpm was observed 3.36, 3.28, and 3.27 kW for D100, DB10, and DP10, respectively. It was observed that the value of the exergy loss rate for D100 was higher than DP10 and DB10. The highest exergy loss rate was 5.4 kW at 3500 rpm, which was obtained for D100. By increasing test engine rpm, the value of exergy destruction rate also increases.

At a given test-engine speed, diesel has had the highest rate of exergy destruction. The value of the exergy destruction rate for D100 was 62.42 kW at 3500 rpm. Exergy destruction values for DP10, DB10, and D100 at 1000 rpm were 58.9, 60.6, and 62.4 kW, respectively. The exergy efficiencies of all considered fuel at different rpm of test engine bed is shown in **Fig. 4**. As the number of engine speed increases, the value of exergy efficiency also increases. At 2000 rpm, the test engine exergy efficiencies are 36.48, 34.98, and 34.78% for DP10, DB10, and D100. The improved exergy efficiency is primarily due to improved air-fuel mixing during combustion and decreased after burn zone [43]. Diesel has a higher calorific value than biodiesel; however, biodiesel has been shown to have higher energetic-exergetic efficiency. Due to various thermodynamic irreversibilities, the engine's exergy efficiency was lower than its energy efficiency [32].

4.3. Thermoeconomic analysis

The test engine was operated with diesel fuel (D100), DP10 and DB10 for thermoeconomic analysis. The detailed results of the thermoeconomic analysis are presented in **Table S4**. The system's capital investment cost was estimated to be $80,000 that the manufacturer gave. As the test engine speed increases, it increases the total energy loss to capital investment value ($R_{en,loss}$). The values of $R_{en,loss}$ of the test engine for D100 were noted as minimum compared to DP10 and DB10 as rpm of the test engine increases. At 1000 rpm, the highest $R_{en,loss}$ value 3.79×10^{-4} kW/$ of the test engine, was observed for DB10, while the lowest value of 3.51×10^{-4} kW/$ was observed D100. An increment in the value of $R_{ex, loss}$ of the test engine was noticed with increasing engine speed. The highest $R_{ex, loss}$ value was D100, and the test engine with the lowest Rex was measured for DP10. At 1000 engine rpm, the $R_{ex, loss}$ values were 2.803×10^{-5} kW/$, 2.728×10^{-5} kW/$ for DB10 and DP10, respectively. The DP10 had lesser $R_{ex, loss}$ as compared to DB10. The increase in the values of $R_{ex, dest}$ of the test engine was spotted as a consequence of the rise in engine speed in this analysis. The higher $R_{ex,dest}$ was noticed when the D100 was used to run the engine. Similarly, the lower $R_{ex,dest}$ was seen when DP10 was used to run the test engine bed.

4.4. Sustainability analysis

Fig. 5 indicates the improvement potential of D100, DP10, and DB10 at different test engine speed. The scope for development of the test engine increases as the rpm of the test engine increases. The maximum values of improvement potential were calculated for D100. The tested fuels improvement potential at 1000 rpm was 20.84, 21.86, and 22.83 kW for DP10, DB10, and D100, respectively. Similarly, the tested fuel improvement potential at 3500 rpm was 35.69, 37.36, 38.91 kW for DP10, DB10, and D100, respectively. When the test engine was fuelled with DP10, the lowest improvement potential levels were calculated at all engine speeds. It is because DP10 had lesser irreversibilities [22]. The tested fuels depletion number variation by increasing the test engine's rpm is shown in **Fig. 6**. As the engine speed increases, the depletion number of the test engine decreases. For DP10, the lowest depletion number was observed. However, the maximum depletion number was obtained for D100. At 1000 rpm, the depletion number was estimated to be 0.79, 0.80, 0.81 for DP10, DB10, and D100, respectively. Similarly, at 3500 rpm, the depletion was estimated to be 0.60, 0.61, 0.62 for DP10, DB10, and D100, respectively.

The effect of test engine speed on the sustainability index of considered fuel is shown in **Fig. 7**. The sustainability index of the fuels tends to increase as the engine speed increases. The highest sustainability index was obtained for DP10. At 1000 rpm, the test engine sustainability index was estimated to be 1.23, 1.24, and 1.26 for D100, DB10, and DP10, respectively. In the same way, at 3500 rpm, the test engine sustainability index was estimated to be 1.60, 1.62 and 1.65 for D100, DB10, and DP10, respectively. Compared to other fuels considered in this analysis, the findings revealed that DP10 was the most sustainable energy source. Karagoz et al. [22] also reported that the DP10 shows the best results compared to other higher blends of TPO-diesel and diesel fuel in energy, exergy, thermoeconomics, and sustainability index in a single-cylinder diesel engine. Yaqoob et al. [44] reported that the DP10 is the best alternative fuel for combustion, performance, and emission.

Moreover, Hurdogan et al. [4] also stated that the DP10 shows the best performance as compared to higher blends of TPO-diesel and diesel fuel.

5. Conclusions

The comparative analysis of the energy, exergy, thermoeconomic, and sustainability of the diesel (D100) and its blend with biodiesel (DB10) and tire pyrolysis oil (DP10) is conducted on the four-cylinder, four strokes, turbocharged common rail direct injection diesel engine. The findings of this study are as follows:

- The highest density value of DP10 offered higher torque and brake power. The calorific value of DP10 is higher than the DB10 and slightly lower than the D100.
- Higher torque value at 3000 rpm offered the highest energy efficiency of DP10 with a value of 37.12%. Similarly, the maximum value of energy efficiency of DB10, D100 was found to be 36.36% and 35.54% at 3000 rpm.
- Higher torque values at 3000 rpm provided the maximum exergy efficiency of the DP10, with a value of 39.60%. At 3000 rpm, the maximum energy efficiency of the DB10 and D100 was determined to be 38.74% and 37.72%, respectively.
- The thermoeconomic analysis shows that the lowest R_{en}, $R_{ex,dest}$, and R_{ex} values were obtained from DP10 at all rpm compared to D100 and DB10, which shows that better thermoeconomic performance was obtained from the test engine will be fueled with DP10.
- Due to the highest energy and exergy efficiency, the DP10 gave the highest sustainability index and lowest improvement potential. Thus, the sustainability analysis shows that the DP10 is the most sustainable fuel compared to D100 and DB10.

Finally, this experimental study's outcome reveals that the DP10 tire pyrolysis oil-diesel blend is suitable for the multi-cylinder diesel engine without any modification due to its tremendous energy, exergy, thermoeconomic, and sustainability index characteristics.

References

[1] Murugan S, Ramaswamy MC, Nagarajan G. A comparative study on the performance, emission and combustion studies of a DI diesel engine using distilled tyre pyrolysis oil-diesel blends. Fuel 2008;87:2111–21. doi:10.1016/j.fuel.2008.01.008.

[2] Wang Y, Dai L, Fan L, Duan D, Liu Y, Ruan R, et al. Microwave-assisted catalytic fast co-pyrolysis of bamboo sawdust and waste tire for bio-oil production. Journal of Analytical and Applied Pyrolysis 2017;123:224–8. doi:10.1016/j.jaap.2016.11.025.

[3] Soni DK, Gupta R. Numerical investigation of emission reduction techniques applied on methanol blended diesel engine. Alexandria Engineering Journal 2016;55:1867–79. doi:10.1016/j.aej.2016.02.019.

[4] Hürdoğan E, Ozalp C, Kara O, Ozcanli M. Experimental investigation on performance and emission characteristics of waste tire pyrolysis oil–diesel blends in a diesel engine. International Journal of Hydrogen Energy 2017;42:23373–8. doi:10.1016/j.ijhydene.2016.12.126.

[5] Jung H, Kittelson DB, Zachariah MR. Characteristics of SME biodiesel-fueled diesel particle emissions and the kinetics of oxidation. Environmental Science and Technology 2006;40:4949–56. doi:10.1021/es0515452.

[6] Behçet R. Performance and emission study of waste anchovy fish biodiesel in a diesel engine. Fuel Processing Technology 2011;92:1187–94. doi:10.1016/j.fuproc.2011.01.012.

[7] Kegl B. Influence of biodiesel on engine combustion and emission characteristics. Applied Energy 2011;88:1803–12. doi:10.1016/j.apenergy.2010.12.007.

[8] He BQ. Advances in emission characteristics of diesel engines using different biodiesel fuels.

Renewable and Sustainable Energy Reviews 2016;60:570–86. doi:10.1016/j.rser.2016.01.093.

[9] Murugan S, Ramaswamy MC, Nagarajan G. Tyre pyrolysis oil as an alternate fuel for diesel engines. SAE International by University of British Columbia, Monday, July 30, 2018, SAE International; 2018, p. 1–6. doi:10.4271/2005-01-2190.

[10] Pilusa TJ. The use of modified tyre derived fuel for compression ignition engines. Waste Management 2017;60:451–9. doi:10.1016/j.wasman.2016.06.020.

[11] Kumaravel ST, Murugesan A, Kumaravel A. Tyre pyrolysis oil as an alternative fuel for diesel engines – A review. Renewable and Sustainable Energy Reviews 2016;60:1678–85. doi:10.1016/j.rser.2016.03.035.

[12] Forrest MJ. Recycling and Re-use of Waste Rubber. De Gruyter; 2019. doi:10.1515/9783110644142.

[13] Williams PT. Pyrolysis of waste tyres: A review. Waste Management 2013;33:1714–28. doi:10.1016/j.wasman.2013.05.003.

[14] Rowhani A, Rainey TJ. Scrap tyre management pathways and their use as a fuel - A review. Energies 2016;9:1–26. doi:10.3390/en9110888.

[15] Siva M, Onenc S, Uçar S, Yanik J. Influence of oily wastes on the pyrolysis of scrap tire. Energy Conversion and Management 2013;75:474–81. doi:10.1016/j.enconman.2013.06.055.

[16] Wang W-C, Bai C-J, Lin C-T, Prakash S. Alternative fuel produced from thermal pyrolysis of waste tires and its use in a DI diesel engine. Applied Thermal Engineering 2016;93:330–8. doi:10.1016/j.applthermaleng.2015.09.056.

[17] Martínez JD, Puy N, Murillo R, García T, Navarro MV, Mastral AM. Waste tyre pyrolysis - A

review. Renewable and Sustainable Energy Reviews 2013;23:179–213. doi:10.1016/j.rser.2013.02.038.

[18] Song W, Zhou J, Li Y, Li S, Yang J. Utilization of waste tire powder for gaseous fuel generation via CO2 gasification using waste heat in converter vaporization cooling flue. Renewable Energy 2021;173:283–96. doi:https://doi.org/10.1016/j.renene.2021.03.090.

[19] Ramos G, Alguacil FJ, López FA. The recycling of end-of-life tyres. Technological review. Revista de Metalurgia 2011;47:273–84. doi:10.3989/revmetalm.1052.

[20] Martínez JD, Rodríguez-Fernández J, Sánchez-Valdepeñas J, Murillo R, García T. Performance and emissions of an automotive diesel engine using a tire pyrolysis liquid blend. Fuel 2014;115:490–9. doi:10.1016/j.fuel.2013.07.051.

[21] Kumar Sharma P, Sharma D, Lal Soni S, Jhalani A, Singh D, Sharma S. Energy, exergy, and emission analysis of a hydroxyl fueled compression ignition engine under dual fuel mode. Fuel 2020;265:116923. doi:10.1016/j.fuel.2019.116923.

[22] Karagoz M, Uysal C, Agbulut U, Saridemir S. Energy, exergy, economic and sustainability assessments of a compression ignition diesel engine fueled with tire pyrolytic oil−diesel blends. Journal of Cleaner Production 2020;264:121724. doi:10.1016/j.jclepro.2020.121724.

[23] Caliskan H, Mori K. Thermodynamic, environmental and economic effects of diesel and biodiesel fuels on exhaust emissions and nano-particles of a diesel engine. Transportation Research Part D: Transport and Environment 2017;56:203–21. doi:https://doi.org/10.1016/j.trd.2017.08.009.

[24] Özdalyan B, Uysal C, Kurt H. Exergy analysis of a spark ignition engine for different crankshaft speeds. Pamukkale University Journal of Engineering Sciences 2019;25:13–9.

doi:10.5505/pajes.2018.81593.

[25] Karthickeyan V, Thiyagarajan S, Ashok B, Edwin Geo V, Azad AK. Experimental investigation of pomegranate oil methyl ester in ceramic coated engine at different operating condition in direct injection diesel engine with energy and exergy analysis. Energy Conversion and Management 2020;205:112334. doi:https://doi.org/10.1016/j.enconman.2019.112334.

[26] Paul A, Panua R, Debroy D. An experimental study of combustion, performance, exergy and emission characteristics of a CI engine fueled by Diesel-ethanol-biodiesel blends. Energy 2017;141:839–52. doi:https://doi.org/10.1016/j.energy.2017.09.137.

[27] Mascarenhas J dos S, Chowdhury H, Thirugnanasambandam M, Chowdhury T, Saidur R. Energy, exergy, sustainability, and emission analysis of industrial air compressors. Journal of Cleaner Production 2019;231:183–95. doi:https://doi.org/10.1016/j.jclepro.2019.05.158.

[28] Chowdhury T, Chowdhury H, Thirugnanasambandam M, Hossain S, Barua P, Ahamed JU, et al. Is the commercial sector of Bangladesh sustainable? – Viewing via an exergetic approach. Journal of Cleaner Production 2019;228:544–56. doi:https://doi.org/10.1016/j.jclepro.2019.04.270.

[29] Aghbashlo M, Tabatabaei M, Mohammadi P, Pourvosoughi N, Nikbakht AM, Goli SAH. Improving exergetic and sustainability parameters of a DI diesel engine using polymer waste dissolved in biodiesel as a novel diesel additive. Energy Conversion and Management 2015;105:328–37. doi:https://doi.org/10.1016/j.enconman.2015.07.075.

[30] Sharma A, Singh Y, Singh NK, Singla A. Sustainability of jojoba biodiesel/diesel blends for DI diesel engine applications- taguchi and response surface methodology concept. Industrial Crops and Products 2019;139:111587. doi:https://doi.org/10.1016/j.indcrop.2019.111587.

[31] Sarıdemir S, Ağbulut Ü. Combustion, performance, vibration and noise characteristics of cottonseed methyl ester–diesel blends fuelled engine. Biofuels 2019;0:1–10. doi:10.1080/17597269.2019.1667658.

[32] Sarıkoç S, Örs İ, Ünalan S. An experimental study on energy-exergy analysis and sustainability index in a diesel engine with direct injection diesel-biodiesel-butanol fuel blends. Fuel 2020;268:117321. doi:10.1016/j.fuel.2020.117321.

[33] Caliskan H, Mori K. Thermodynamic, environmental and economic effects of diesel and biodiesel fuels on exhaust emissions and nano-particles of a diesel engine. Transportation Research Part D: Transport and Environment 2017;56:203–21. doi:10.1016/j.trd.2017.08.009.

[34] Madhankumar S, Viswanathan K, Wu W. Energy, exergy and environmental impact analysis on the novel indirect solar dryer with fins inserted phase change material. Renewable Energy 2021;176:280–94. doi:10.1016/j.renene.2021.05.085.

[35] Kotas TJ. The Exergy Method of Thermal Plant Analysis. 1985.

[36] Adrian Bejan, George Tsatsaronis MJM. Thermal Design and Optimization. 1996.

[37] Rosen MA, Dincer I. Exergy–cost–energy–mass analysis of thermal systems and processes. Energy Conversion and Management 2003;44:1633–51. doi:https://doi.org/10.1016/S0196-8904(02)00179-6.

[38] Rosen MA, Dincer I, Kanoglu M. Role of exergy in increasing efficiency and sustainability and reducing environmental impact. Energy Policy 2008;36:128–37. doi:10.1016/j.enpol.2007.09.006.

[39] Van Gool W. Energy Policy: Fairy Tales and Factualities BT - Innovation and Technology — Strategies and Policies. Innovation and Technology — Strategies and Policies, 1997, p. 93–

105.

[40] Connelly L, Koshland CP. Two aspects of consumption: Using an exergy-based measure of degradation to advance the theory and implementation of industrial ecology. Resources, Conservation and Recycling 1997;19:199–217. doi:10.1016/S0921-3449(96)01180-9.

[41] Chintala V, Subramanian KA. Assessment of maximum available work of a hydrogen fueled compression ignition engine using exergy analysis. Energy 2014;67:162–75. doi:https://doi.org/10.1016/j.energy.2014.01.094.

[42] Pote RN, Patil RK. Combustion and emission characteristics analysis of waste tyre pyrolysis oil. SN Applied Sciences 2019;294. doi:10.1007/s42452-019-0308-8.

[43] Karthickeyan V. Effect of combustion chamber bowl geometry modification on engine performance, combustion and emission characteristics of biodiesel fuelled diesel engine with its energy and exergy analysis. Energy 2019;176:830–52. doi:10.1016/j.energy.2019.04.012.

[44] Yaqoob H, Teoh YH, Jamil MA, Gulzar M. Potential of tire pyrolysis oil as an alternate fuel for diesel engines: A review. Journal of the Energy Institute 2021;96:1–17. doi:https://doi.org/10.1016/j.joei.2021.03.002.

List of Tables

Table 1. The properties of diesel fuel, neat tire pyrolysis oil, neat biodiesel, and their blends.

Fuel type	Density (g/L)	Lower heating value (MJ/kg)	Cetane number
Diesel (D100)	833.70	45.63	52
DB10	836.30	44.68	55
DP10	849.00	44.81	49
Neat Tire Pyrolysis Oil (P100)	973.60	41.60	29
Neat Biodiesel (B100)	875.50	38.89	61

Table 2. Engine test bed parameters and specifications.

Parameters	Specifications
Model	Renault Kangoo K9K 700 model engine
Type	Diesel turbocharged engine
Fuel injection system	Common-rail direct injection system
No. of cylinders	4
Strokes	4
Valves/cylinder	2
Maximum power	48 kW @ 4000 rpm
Bore x stroke	76.0 x 80.5 mm
Maximum torque	160 Nm @ 2000 rpm
Total cylinder volume	1.461 L
Compression ratio	18.25: 1
Emission certification	Euro-II

Table 3. Detail of measurement type, range, accuracy, technique, and percentage uncertainty.

Measurement type	Range	Accuracy	Technique	Uncertainty (%)
Load	±600 Nm	±0.1 Nm	Strain gauge type load cell	±0.25
Engine Speed	0-10,000 rpm	±1 rpm	Magnetic pick-up type	±0.10
Fuel flow	0.5-36 L/hr	±0.04 L/hr	Positive displacement gear wheel flow meter	±0.50
Air flow	0.25-7.83 kg/min	±0.07 kg/min	Hot wire air mass meter	±2
CO emission	0-10% volume	±0.001%	Non-dispersive infrared	±1
CO_2 emission	0-10% volume	±0.001%	Non-dispersive infrared	±1
NO_x emission	0-5,000 ppm	±1 ppm	Electrochemical	±1.30
Pressure	0-25,000 kPa	±10 kPa	Piezoelectric crystal type	±0.50
Temperature	0-1200 °C	±0.3 °C	Thermocouple (Type K)	±0.15
Calculated				
$E\dot{n}_{air}$		±0.04 kW		±0.30
$E\dot{n}_{fuel}$		±0.31 kW		±0.40
$E\dot{n}_{w}$		±0.11 kW		±0.26
$E\dot{n}_{exh}$		±0.019 kW		±0.40
$E\dot{n}_{loss}$		±0.36 kW		±0.50
η_{en}		±0.14%		±0.40
$E\dot{x}_{air}$		±0.00016 kW		±0.61
$E\dot{x}_{fuel}$		±0.340 kW		±0.29
$E\dot{x}_{w}$		±0.110 kW		±0.26
$E\dot{x}_{exh}$		±0.015 kW		±0.52
$E\dot{x}_{loss}$		±0.027 kW		±0.50
$E\dot{x}_{dest}$		±0.32 kW		±0.52
ψ_{ex}		±0.15%		±0.40

$R_{en,loss}$	±0.0000045 (kW/$)	±0.50
$R_{ex,loss}$	±0.00000034 (kW/$)	±0.50
$R_{ex,dest}$	±0.000004 (kW/$)	±0.51

Table 4. The mass fractions of oxygen, carbon, hydrogen, and sulfur of considered fuels.

	O (%)	C (%)	H (%)	α (%)
Diesel	0.01	86.58	13.29	0.11
DP10	0.63	86.14	13.07	0.04
DB10	0.83	86.15	12.92	0.09

Table 5. Environmental molar fractions of exhaust gases [36].

Elements	Molar Fractions (%)
N_2	75.6700
CO	0.00070
CO_2	0.03450
H_2O	3.03000
H_2	0.00005
SO_2	0.00020
O_2	20.3500
Others	0.91455

List of Figures

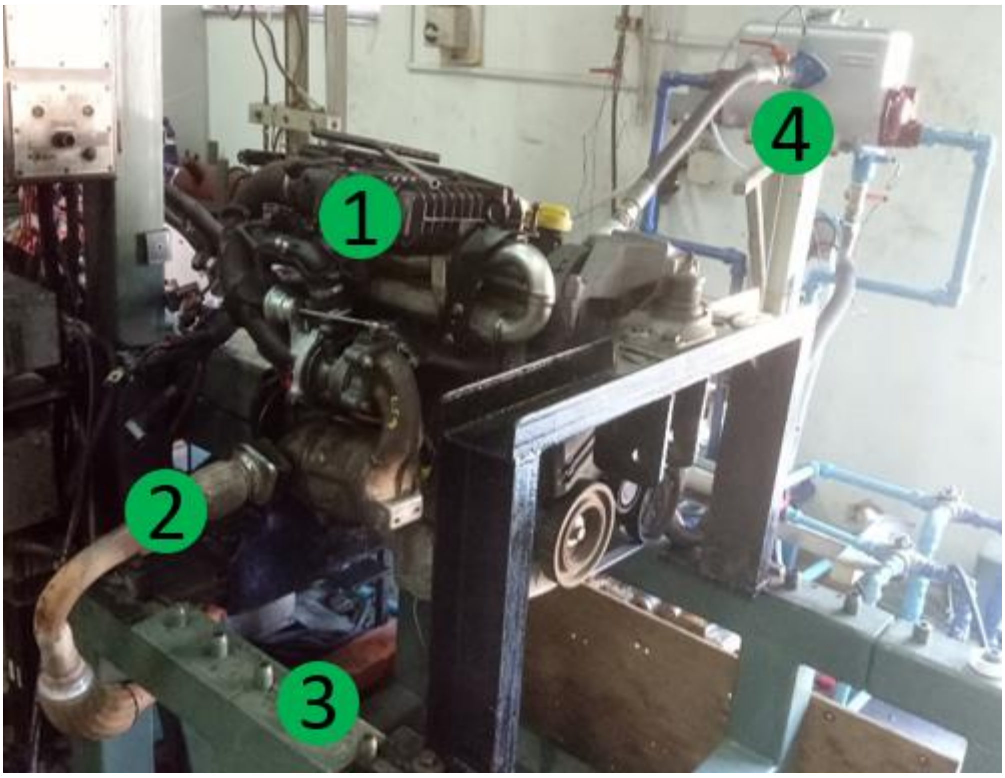

Fig. 1. Experimental setup; (1) Engine, (2) Muffler, (3) Test bed and (4) Engine cooling system (Heat exchanger).

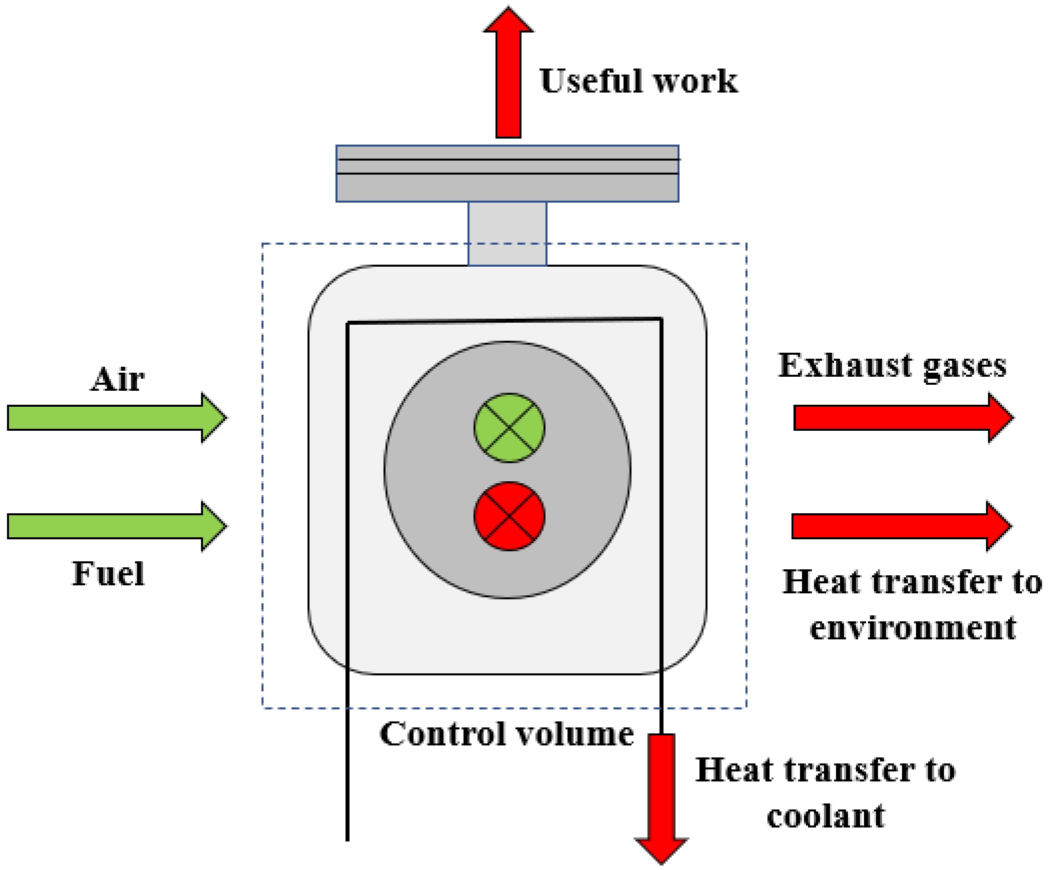

Fig. 2. Thermodynamic energy balance diagram for control volume [25].

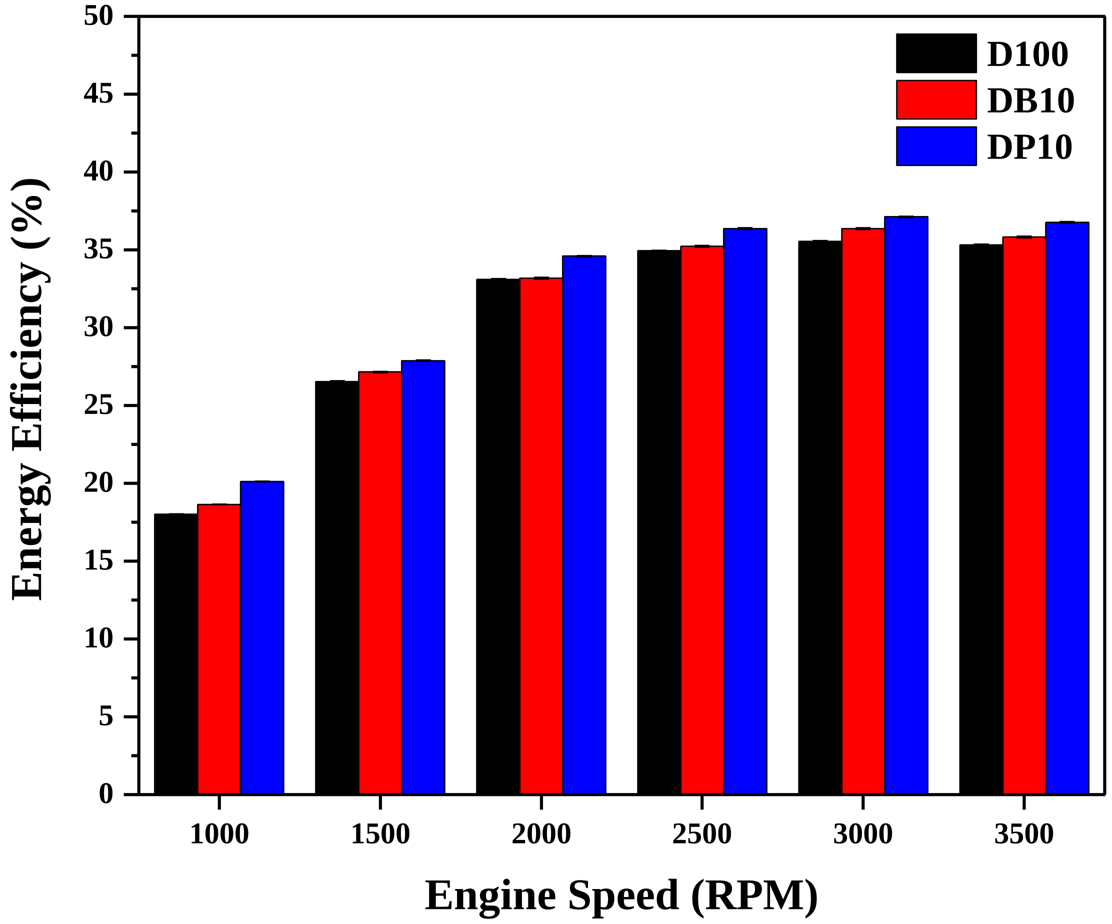

Fig. 3. The energy efficiency of the different tested fuels at various engine speeds.

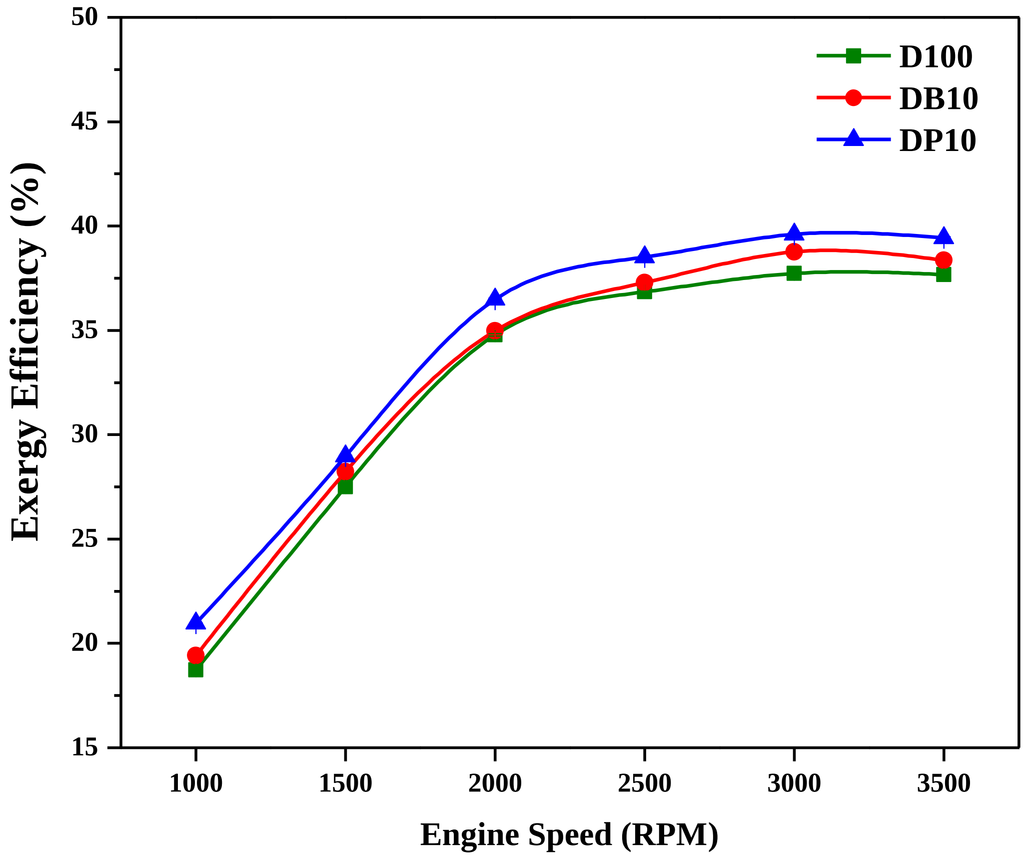

Fig. 4. The exergy efficiency of the different tested fuels at various engine speeds.

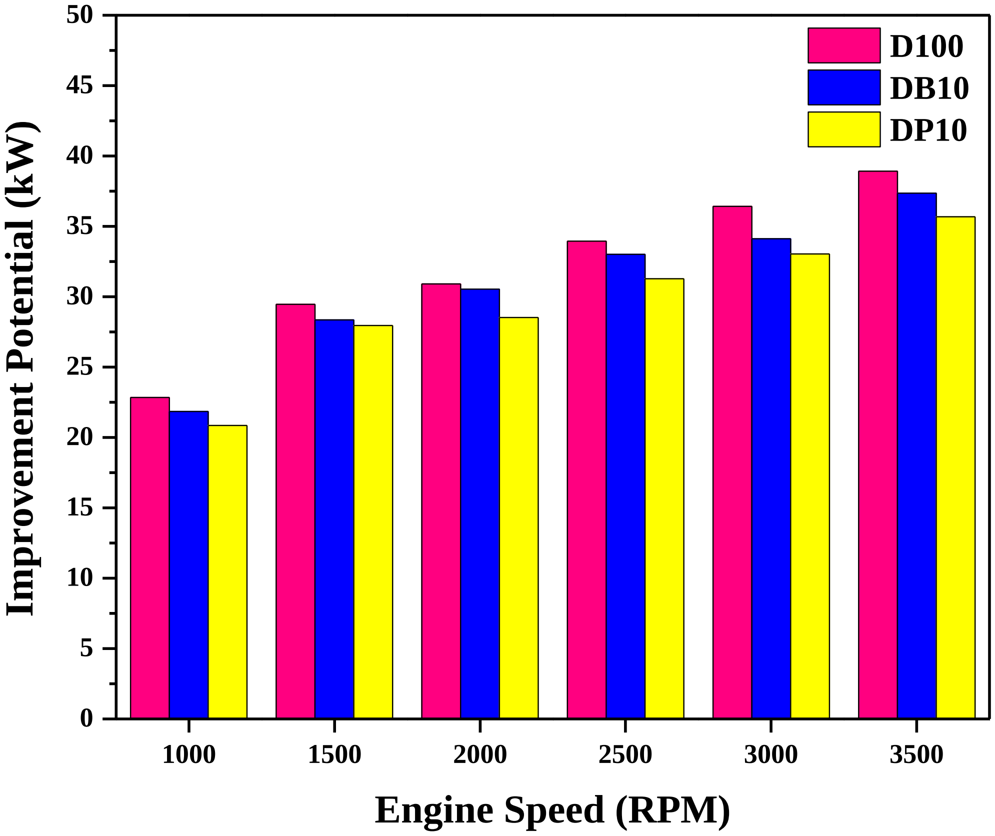

Fig. 5. The improvement potential of the different tested fuels at various engine speeds.

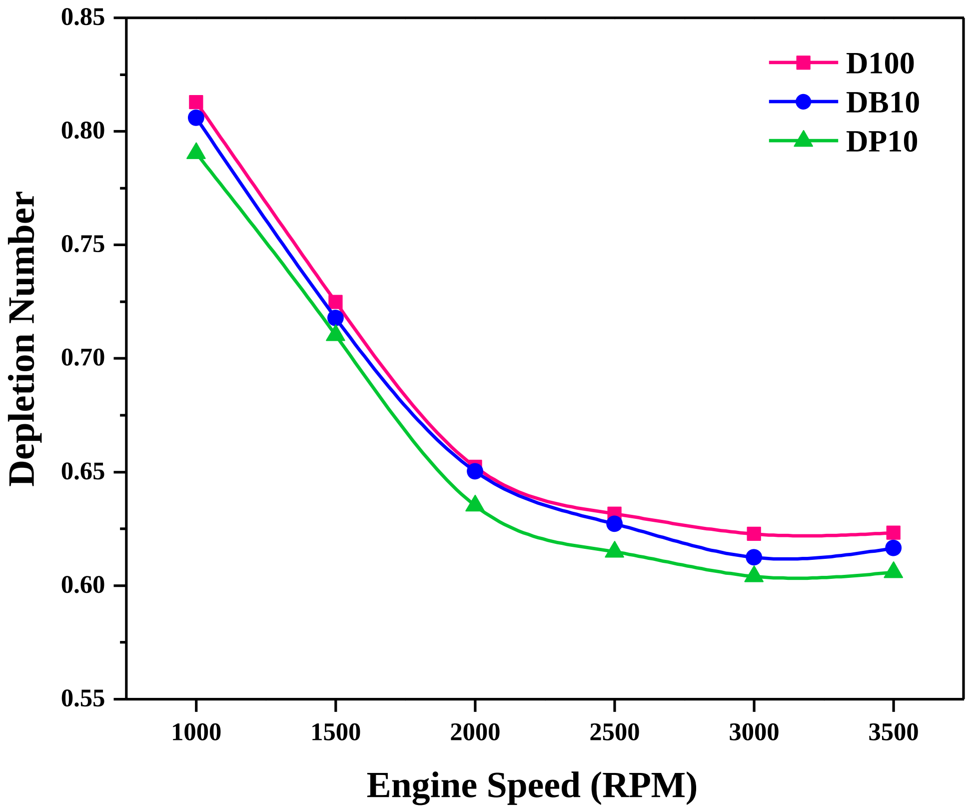

Fig. 6. The depletion number of the different tested fuels at various engine speeds.

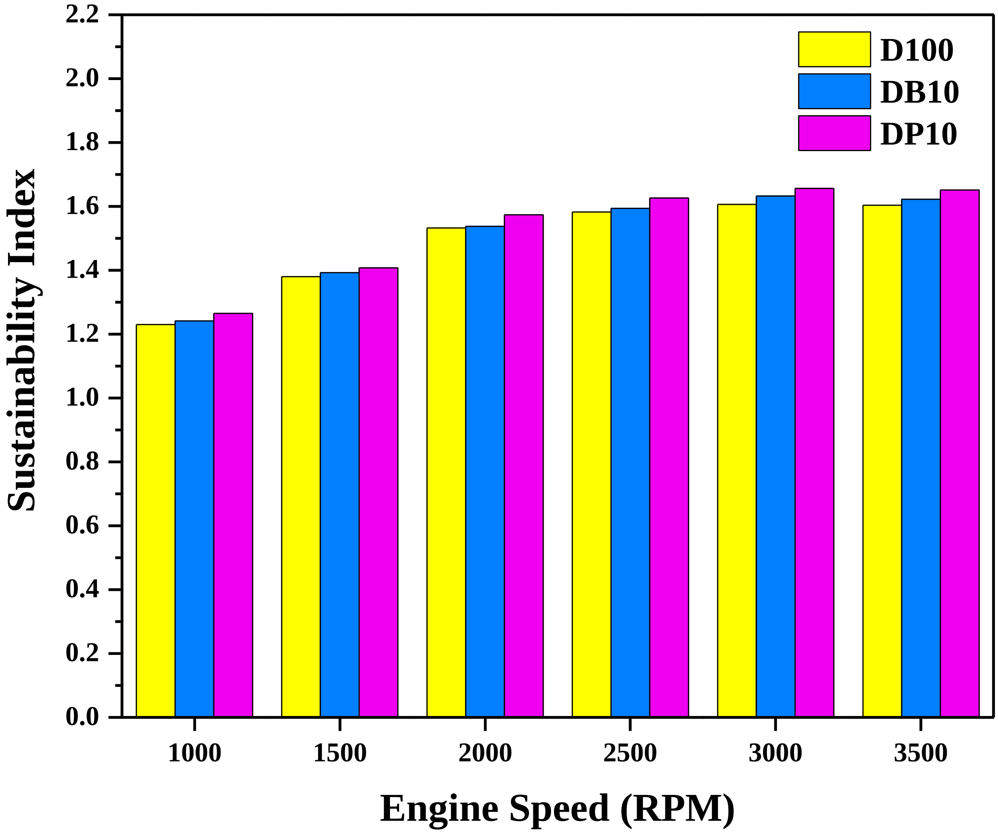

Fig. 7. The sustainability index of the different tested fuels at various engine speeds.